Two-level correlation function of critical random-matrix ensembles

E. Cuevas
Departamento de Física, Universidad de Murcia, E-30071 Murcia, Spain.
(Dated: February 2, 2008)

The two-level correlation function $R_{d,\beta}(s)$ of d-dimensional disordered models ($d = 1$, 2, and 3) with long-range random-hopping amplitudes is investigated numerically at criticality. We focus on models with orthogonal ($\beta = 1$) or unitary ($\beta = 2$) symmetry in the strong ($b^d \ll 1$) coupling regime, where the parameter b^{-d} plays the role of the coupling constant of the model. It is found that $R_{d,\beta}(s)$ is of the form $R_{d,\beta}(s) = 1+\delta(s)-F_\beta(s^\beta/b^{d\beta})$, where $F_1(x) = \mathrm{erfc}(a_{d,\beta}\, x)$ and $F_2(x) = \exp(-a_{d,\beta}\, x^2)$, with $a_{d,\beta}$ being a numerical coefficient depending on the dimensionality and the universality class. Finally, the level number variance and the spectral compressibility are also considerded.

PACS numbers: 71.30.+h, 72.15.Rn, 71.55.Jv, 05.40.-a

I. INTRODUCTION

Random-matrix theories are largely and successfully applied in the theoretical description of complex nuclei[1,2], gauge field theories,[3,4,5] mesoscopic systems,[6,7,8,9] and random surfaces in the field of quantum gravity.[10] Their advantage is that it is possible to represent the Hamiltonian of the corresponding system by a large Hermitian matrix acting on a finite-dimensional Hilbert space (if one disregards the continuous part of the spectrum).

The random matrices fall into one of three universality classes, named orthogonal ($\beta = 1$), unitary ($\beta = 2$), and symplectic ($\beta = 4$), depending on the global symmetry properties of the Hamiltonian they represent.[11] The symmetry parameter β is the number of independent real components that characterizes a matrix element of the Hamiltonian. A system belongs to the orthogonal class if it has both time-reversal and spin-rotation symmetries, to the unitary class if time-reversal symmetry is broken, and to the symplectic class if the system has time-reversal symmetry but spin-rotation is broken. The relevant terms in the Hamiltonian are a coupling to an applied magnetic field, which breaks time-reversal symmetry, and the spin-orbit interaction, which breaks spin-rotation symmetry.

One of the most relevant applications of the random matrix ensembles is to the study of critical phenomena, particularly to the special case of critical statistics which is found at the Anderson metal-insulator transition (MIT) in disordered systems.[12,13,14,15,16,17,18,19,20,21,22,23,24,25] At the critical point, the states acquire the property of multifractality, which marks a qualitative difference from the extended states in a metal and localized states in an insulator. These critical states correspond to critical-level statistics. Although several ensembles of nonconventional random matrices have been suggested to describe this statistics[26,27,28,29,30,31,32] we wish to emphasize the power-law random-banded matrix model (PRBM),[33] for which the multifractality of eigenstates has been rigorously proven.[33,34] This model is characterized by a variance of their off-diagonal matrix elements, which decay as a power law with increasing distance from the diagonal. It should be mentioned that all these models are of a one-dimensional nature.

Energy-level correlations provide general tools for the statistical description of disordered systems, helping in our understanding of the localization transition. An important statistical measure of spectral correlations is the two-level correlation function (TLCF) of the density of states (DOS), which measures the correlations of the DOS at two different energies. This function has been derived analytically for the PRBM model in the two limiting cases of weak and strong disorder by mapping the corresponding Hamiltonian onto an effective σ model of a one-dimensional (1D) nature[35] and using renormalization-group methods,[36,37] respectively. We stress that, unlike the 1D PRBM model, it has not until now been possible to analytically solve the most interesting, from an experimental point of view, disordered models with long-range transfer terms in $d = 2$ and 3. Thus, explicit results for the TLCF in two-dimensional (2D) and three-dimensional (3D) models are still lacking, and finding this function is essential in order to fully understand the MITs. For this reason, we addressed the problem using numerical calculations. An important and closely related quantity, the level-number variance (LNV), will be also considered.

In this work we numerically calculate the TLCF and the LNV of critical d-dimensional random matrix ensembles with long-range off-diagonal elements and orthogonal or unitary symmetry. Since MITs generically take place at strong disorder (conventional Anderson transition, quantum Hall transition, transition in $d = 2$ for electrons with strong spin-orbit coupling, etc.), we will restrict ourselves to the study of both quantities in this regime. In the 1D case our results for the TLCF are in good agreement, except for the numerical coefficient, with existing analytical estimates.[35] In addition, we propose expressions for the TLCF in the $d = 2$ and 3 cases. Apart from the importance of these findings from a general point of view, they may be relevant for several real physical systems (see Sec. II).

The paper begins by first describing the model and the methods used for the calculations in Sec. II. The results for the TLCF and the LNV in models with orthogonal or unitary symmetry are presented in Secs. III and IV, respectively. Finally, Sec. V summarizes our findings.

II. MODEL AND METHODS

In order to fully represent the mesoscopic systems we introduce an explicit dependence on dimensionality d in the widely

studied PRBM ensemble.[33,34,35,38,39,40,41,42,43,44,45,46,47,48,49,50] Thus, we consider a generalization to d dimensions of this ensemble. The corresponding Hamiltonian, which describes noninteracting electrons on a disordered d-dimensional square lattice with random long-range hopping, is represented by random Hermitian $L^d \times L^d$ matrices $\widehat{\mathcal{H}}$ (real for $\beta = 1$ or complex for $\beta = 2$), whose entries are randomly drawn from a normal distribution with zero mean, $\langle \mathcal{H}_{ij} \rangle = 0$, and a variance that depends on the distance between the lattice sites $\boldsymbol{r}_i$

$$\left\langle |\mathcal{H}_{ij}|^2 \right\rangle = \frac{1}{1 + (|\boldsymbol{r}_i - \boldsymbol{r}_j|/b)^{2\alpha}} \times \begin{cases} \frac{1}{2\beta} \ , & i \neq j \\ \frac{1}{\beta} \ , & i = j \end{cases} \qquad (1)$$

in which standard Gaussian ensemble normalization is used.[51]

Using field-theoretical methods,[26,33,34,36,38,39,52,53] the PRBM model was shown to undergo a sharp transition at $\alpha = d$ from localized states for $\alpha > d$ to delocalized states for $\alpha < d$. This transition shows all the key features of the Anderson MIT, such as multifractality of the eigenfunctions and nontrivial spectral compressibility at criticality. In what follows, we focus on the critical value $\alpha = d$.

The parameter b^d in Eq. (1) is an effective bandwidth that serves as a continuous control parameter over a whole line of criticality, i.e, for an exponent equal to d in the hopping elements $\mathcal{H}_{ij} \sim b^d$.[36] Furthermore, it determines the critical dimensionless conductance in the same way as the dimensionality labels the different Anderson transitions. Each regime is characterized by its respective coupling strength, which depends on the ratio $(\langle |\mathcal{H}_{ii}|^2 \rangle / \langle |\mathcal{H}_{ij}|^2 \rangle)^{1/2} \propto b^{-d}$ between diagonal disorder and the off-diagonal transition matrix elements of the Hamiltonian.[54]

Many real systems of interest can be described by Hamiltonians (1). Among such systems are optical phonons in disordered dielectric materials coupled by electric dipole forces,[55] excitations in two-level systems in glasses interacting via elastic strain,[56] magnetic impurities in metals coupled by an r^{-3} Ruderman-Kittel-Kasuya-Yodida interaction,[57] and impurity quasiparticle states in two-dimensional disordered d-wave superconductors.[58] It also describes a particle moving fast through a lattice of Coulomb scatterers with power-law singularity,[53] the dynamics of two interacting particles in a 1D random potential,[59] and a quantum chaotic billiard with a nonanalytic boundary.[60]

The TLCF is defined in the usual way

$$R_{d,\beta}(\omega) = \frac{1}{\langle \nu(\epsilon) \rangle^2} \langle \nu(\epsilon + \omega/2) \nu(\epsilon - \omega/2) \rangle \ , \qquad (2)$$

where $\nu(\epsilon) = L^{-d} \mathrm{Tr}\, \delta(\epsilon - \widehat{\mathcal{H}})$ is the fluctuating DOS and $\langle \ \rangle$ denotes averaging over disorder realizations. At the critical point $R_{d,\beta}(\omega)$ acquires a scale-invariant form, if considered as a function of $s = \omega/\Delta$, the frequency normalized to the mean level spacing $\Delta = 1/L^d \langle \nu(\epsilon) \rangle$.[12,13,14] In the case of constant average DOS, $R_{d,\beta}(s = \omega/\Delta)$ can be simply rewritten as

$$R_{d,\beta}(s) = \delta(s) + \sum_n p(n; s) \ , \qquad (3)$$

where $p(n; s)$ is the distribution of distances s_n between n other energy levels and the $\delta(s)$ function describes the self-correlation of the levels.[11]

The strong disorder limit ($b \ll 1$) of the 1D PRBM model can be studied using the renormalization-group method of Refs. 36 and 37. For orthogonal symmetry, the following result is obtained for the TLCF at the center of the spectral band:[35]

$$R_{1,1}(s) = 1 + \delta(s) - \mathrm{erfc}\left(a_{1,1} \frac{|s|}{b} \right) \ , \qquad (4)$$

where $\mathrm{erfc}(x) = (2/\sqrt{\pi}) \int_x^\infty \exp(-t^2) dt$ is the complementary error function and $a_{1,1} = 1/\sqrt{\pi}$, whereas for unitary symmetry

$$R_{1,2}(s) = 1 + \delta(s) - \exp\left(-a_{1,2} \frac{s^2}{b^2} \right) \qquad (5)$$

with $a_{1,2} = 2/\pi$. Note that for small s, $R_{1,\beta}(s)$ behave as s^β thus reflecting the levels repulsion effect, whereas they tend asymptotically to 1 at large values of s.

Another important quantity, which characterizes fluctuations in the level density on larger scales than the mean spacing, is the variance

$$\Sigma^2_{d,\beta}(\langle n \rangle) = \langle n^2 \rangle - \langle n \rangle^2 \qquad (6)$$

of the number of levels in an energy window that contains $1 \ll \langle n \rangle \ll N$ on average. This variance is given in terms of the TLCF by $\Sigma^2_{d,\beta}(\langle n \rangle) = \int_{-\langle n \rangle}^{\langle n \rangle} (\langle n \rangle - |s|) R_{d,\beta}(s)\, ds$. The number variance (6) is a statistical quantity that provides a quantitative measure of the long-range rigidity of the energy spectrum. For the Poisson distribution, the levels are uncorrelated and there are large level-number fluctuations, leading to a linear variance $\Sigma^2_{d,\beta}(\langle n \rangle) = \langle n \rangle$. On the other hand, the level correlations in the Wigner-Dyson statistics make the spectrum more rigid and the number variance grows only logarithmically $\Sigma^2_{d,\beta}(\langle n \rangle) \sim \ln\langle n \rangle$. However, in the critical regime, the variance has been conjectured to be Poisson-like[12,16,17]

$$\Sigma^2_{d,\beta}(\langle n \rangle) \sim \chi \langle n \rangle \ , \qquad (7)$$

where the level compressibility χ is another important parameter for characterizing the MIT and which takes values $0 \leq \chi \leq 1$, with zero referring to delocalized states and unity the localized states.

For the computation of $R_{d,\beta}(s)$ and $\Sigma^2_{d,\beta}(\langle n \rangle)$, we unfold the spectrum in each case to a constant density and rescale it so as to have the mean spacing equal to unity. Then we calculate $p(n; s)$ and use Eqs. (3) and (6), respectively. The system sizes range between $L = 500$ and 6000 in 1D, $L = 20$ and 100 in 2D, and between 8 and 14 in 3D, whereas b^d ranges in the interval $0.02 \leq b^d \leq 0.12$. We consider a small energy window, containing about 10% of the states around the center of the band. The number of random realizations is such that the number of critical levels included for each L is roughly 1.2×10^6. In order to reduce edge effects, periodic boundary conditions are included.

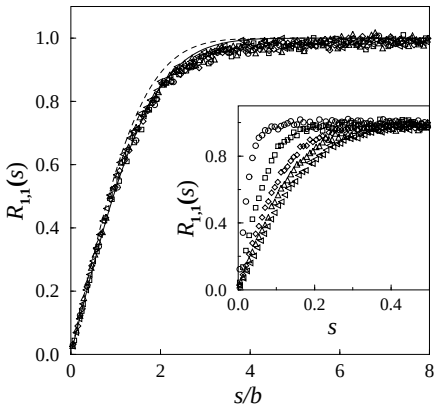

FIG. 1: $R_{1,1}(s)$ for the 1D model (1) with orthogonal symmetry ($\beta = 1$) as a function of the rescaled variable s/b at different b values for several system sizes: $b = 0.02, L = 4000$ (circles), $b = 0.05, L = 6000$ (squares), $b = 0.08, L = 1000$ (diamonds), $b = 0.1, L = 4000$ (up triangles), and $b = 0.12, L = 1000$ (left triangles). The solid and dashed lines represent the renormalization-group estimate [Eq. (4)], with the fitting parameter $a_{1,1} = 0.502$ and the predicted $a_{1,1} = 1/\sqrt{\pi}$, respectively. The inset shows the same data on the scale s.

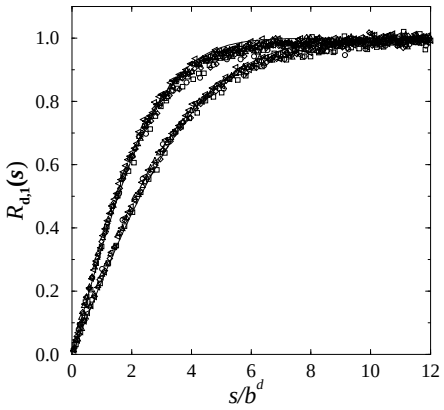

FIG. 2: $R_{d,1}(s)$ for the 2D (upper curve) and 3D (lower curve) models with orthogonal symmetry $\beta = 1$ as a function of the rescaled variable s/b^d at different b^d values for several system sizes: $b^2 = 0.02, L^2 = 40^2$ (circles), $b^2 = 0.05, L^2 = 20^2$ (squares), $b^2 = 0.08, L^2 = 60^2$ (diamonds), $b^2 = 0.1, L^2 = 100^2$ (up triangles), $b^2 = 0.12, L^2 = 30^2$ (left triangles), $b^3 = 0.02, L^3 = 12^3$ (circles), $b^3 = 0.05, L^3 = 14^3$ (squares), $b^3 = 0.08, L^3 = 12^3$ (diamonds), $b^3 = 0.1, L^3 = 8^3$ (up triangles), and $b^3 = 0.12, L^3 = 10^3$ (left triangles). The solid lines are fits to Eq. (8), with the fitting parameters $a_{2,1} = 0.308$ and $a_{3,1} = 0.208$.

III. TWO-LEVEL CORRELATION FUNCTION

In this section, we numerically compute the TLCF $R_{d,\beta}(s)$ of Hamiltonians (1) with the orthogonal or unitary symmetry for different values of the inverse coupling constant $b^d \ll 1$ and various system sizes. We also compare our results with the analytical estimates of Ref. 35 for the 1D model.

A. Orthogonal symmetry

Let us first check the renormalization-group result, Eq. (4), corresponding to the 1D Hamiltonian (1) with orthogonal symmetry $\beta = 1$. The inset of Fig. 1 displays our results for $R_{1,1}(s)$ at different b values for several system sizes: $b = 0.02, L = 4000$ (circles), $b = 0.05, L = 6000$ (squares), $b = 0.08, L = 1000$ (diamonds), $b = 0.1, L = 4000$ (up triangles), and $b = 0.12, L = 1000$ (left triangles). If the horizontal axis is rescaled by a factor $1/b$, then all data should collapse onto a single curve. The main panel of Fig. 1 shows $R_{1,1}(s)$ as a function of the rescaled variable s/b, thus, confirming the s/b dependence of $R_{1,1}(s)$. The best fit of this data set to Eq. (4) gives the fitting parameter $a_{1,1} = 0.502 \pm 0.003$, which is smaller than the predicted value $1/\sqrt{\pi} = 0.564$. Reference 35 reported numerical values of $R_{1,1}(s)$ at $b = 0.1$ for two small system sizes $L = 256$ and 512, and, as in our calculations, their results were also in relative disagreement with the value $1/\sqrt{\pi}$ in Eq. (4). The solid and dashed lines represent Eq. (4), with the fitting parameter $a_{1,1} = 0.502$ and the predicted $a_{1,1} = 1/\sqrt{\pi}$, respectively. Note that in Ref. 35 a different normalization was used in Eq. (1).

Next we consider the $d = 2$ and 3 cases for which, as mentioned in the Introduction, there are no analytical predictions. The results for $R_{d,1}(s)$ are shown in Fig. 2 in which we were able to collapse both sets of data onto single curves by rescaling the normalized spacing s to the coupling constant $1/b^d$ of the model. Given the similarity of these results with those for the 1D model, a curve of the form

$$R_{d,1}(s) = 1 + \delta(s) - \text{erfc}\left(a_{d,1}\,\frac{|s|}{b^d}\right) \qquad (8)$$

was fitted to the data points in this graph and found that $a_{2,1} = 0.308 \pm 0.001$ and $a_{3,1} = 0.208 \pm 0.001$. These fits are represented as solid lines in Fig. 2. Thus, the system dimensionality d of the TLCF enters via the inverse-coupling constant b^{-d}. We stress that Eq. (8) gives a fairly good fit to the data. The reported data correspond to $b^2 = 0.02, L^2 = 40^2$ (circles), $b^2 = 0.05, L^2 = 20^2$ (squares), $b^2 = 0.08, L^2 = 60^2$ (diamonds), $b^2 = 0.1, L^2 = 100^2$ (up triangles), $b^2 = 0.12, L^2 = 30^2$ (left triangles), $b^3 = 0.02, L^3 = 12^3$ (circles), $b^3 = 0.05, L^3 = 14^3$ (squares), $b^3 = 0.08, L^3 = 12^3$ (diamonds), $b^3 = 0.1, L^3 = 8^3$ (up triangles), and $b^3 = 0.12, L^3 = 10^3$ (left triangles).

These results allow us to generalize the 1D analytical result [Eq. (4)] to the 2D and 3D models by simply replacing the inverse-coupling constant b of the $1d$ case by the corresponding to the d-dimensional case b^d.

The observed b^d dependence of $R_{d,1}(s)$ in Eq. (8) is not surprising since other critical properties, such as the correlation dimension d_2 in 1D and 2D present a similar behavior toward b^d. Specifically, $d_2 = 1 - 1/\pi b$ ($b \gg 1$) and $d_2 = 2b$ ($b \ll 1$) were derived in Refs. 33 and 34, whereas $d_2 = 2 - a_2/b^2$ ($b^2 \gg 1$) and $d_2 = c_2 b^2$ ($b^2 \ll 1$) were numerically found in Ref. 61.

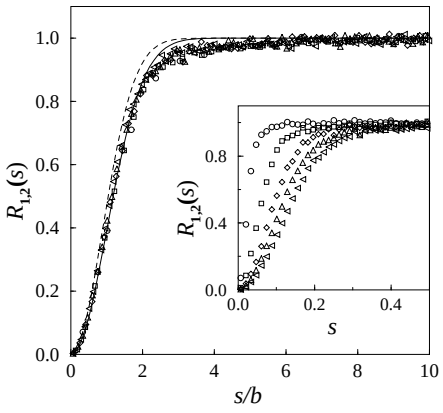

FIG. 3: As in Fig. 1, for the 1D model (1) with unitary symmetry ($\beta = 2$). Data correspond to $b = 0.02, L = 500$ (circles), $b = 0.05, L = 1000$ (squares), $b = 0.08, L = 2000$ (diamonds), $b = 0.1, L = 500$ (up triangles), and $b = 0.12, L = 1000$ (left triangles). The solid and dashed lines represent Eq. (5), with the fitting parameter $a_{1,2} = 0.495$ and the predicted $a_{1,2} = 2/\pi$, respectively. The inset shows the same data on the scale s.

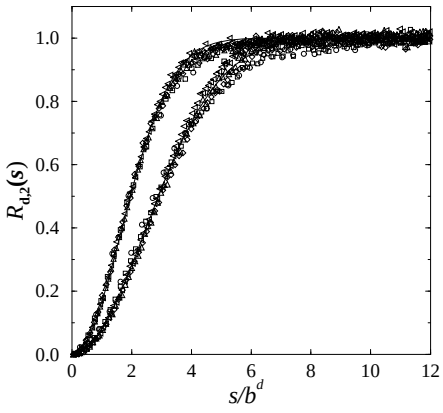

FIG. 4: As in Fig. 2, for the 2D (upper curve) and 3D (lower curve) models with unitary symmetry ($\beta = 2$). Data correspond to $b^2 = 0.02, L^2 = 40^2$ (circles), $b^2 = 0.05, L^2 = 20^2$ (squares), $b^2 = 0.08, L^2 = 60^2$ (diamonds), $b^2 = 0.1, L^2 = 80^2$ (up triangles), $b^2 = 0.12, L^2 = 30^2$ (left triangles), $b^3 = 0.03, L^3 = 12^3$ (circles), $b^3 = 0.05, L^3 = 14^3$ (squares), $b^3 = 0.08, L^3 = 10^3$ (diamonds), $b^3 = 0.1, L^3 = 10^3$ (up triangles), and $b^3 = 0.12, L^3 = 8^3$ (left triangles). The solid lines are fits to Eq. (8), with the fitting parameter $a_{2,2} = 0.181$ and $a_{3,2} = 0.083$, respectively.

B. Unitary symmetry

As in Sec. III A we first analyze the 1D case in order to compare the numerical data with the analytical result [Eq. (5)]. Figure 3 shows $R_{1,2}(s)$ as a function of the rescaled variable s/b. As expected, all data points collapse onto the same curve. The inset displays the same data on the s scale. The values of b and L reported are: $b = 0.02, L = 500$ (circles), $b = 0.05, L = 1000$ (squares), $b = 0.08, L = 2000$ (diamonds), $b = 0.1, L = 500$ (up triangles), and $b = 0.12, L = 1000$ (left triangles). Fitting these data to Eq. (5) gives $a_{1,2} = 0.495 \pm 0.005$, which again is small that the predicted value $2/\pi = 0.637$. To our knowledge, this is the first numerical confirmation of Eq. (5). The solid and dashed lines represents Eq. (5), with the fitting parameter $a_{1,2} = 0.495$ and the predicted $a_{1,2} = 2/\pi$, respectively.

The results for $R_{d,2}(s)$ in the $d = 2$ and 3 models are shown in Fig. 4, in which one can clearly appreciate the collapse of both sets of data when represented as a function of the rescaled variable s/b^d. As in the cases of $\beta = 1$, a curve of the form

$$R_{d,2}(s) = 1 + \delta(s) - \exp\left(-a_{d,2}\,\frac{s^2}{b^{2d}}\right) \qquad (9)$$

was fitted to the data points in this graph, where $a_{d,\beta}$ is a fitting parameter. The data reported correspond to $b^2 = 0.02, L^2 = 40^2$ (circles), $b^2 = 0.05, L^2 = 20^2$ (squares), $b^2 = 0.08, L^2 = 60^2$ (diamonds), $b^2 = 0.1, L^2 = 80^2$ (up triangles), $b^2 = 0.12, L^2 = 30^2$ (left triangles), $b^3 = 0.03, L^3 = 12^3$ (circles), $b^3 = 0.05, L^3 = 14^3$ (squares), $b^3 = 0.08, L^3 = 10^3$ (diamonds), $b^3 = 0.1, L^3 = 10^3$ (up triangles), and $b^3 = 0.12, L^3 = 8^3$ (left triangles). The solid lines in Fig. 4 are fits to Eq. (9) with fitting parameters $a_{2,2} = 0.181 \pm 0.001$ and $a_{3,2} = 0.083 \pm 0.001$. Note that this equation gives a fairly good fit to the data.

For the system sizes considered ($L^d \gg 1$) we have checked that $R_{d,\beta}(s)$ is an L-independent universal scale-invariant function, thus confirming the existence of a critical distribution exactly at the transition. Furthermore, using the nearest-level distribution $p(0; s)$, we verified that the normalized nearest level variances are indeed scale invariant at each critical point studied.[62]

Before concluding the section, we summarize in Table I the nonuniversal constants $a_{d,\beta}$ found. Note that each value is different for every d and β, thus reflecting its dependence on the Hamiltonian symmetry and dimensionality. The values in brackets were obtained from the spectral compressibility (see Sec. IV).

IV. LEVEL NUMBER VARIANCE

This section is devoted to the calculation of the LNV $\Sigma^2_{d,\beta}(\langle n\rangle)$ and the spectral compressibility χ of models (1) with the orthogonal or unitary symmetry in the strong coupling regimen, $b^d \ll 1$. Our results for χ are compared with the analytical prediction of Ref. 63.

It is well known that the statistical properties of spectra of disordered one-electron systems are closely related

TABLE I: Nonuniversal constants $a_{d,\beta}$ of the TLCF. The values in brackets were obtained from the spectral compressibility.

	$d = 1$	2	3
$\beta = 1$	0.502 (0.497)	0.308 (0.291)	0.208 (0.232)
2	0.495 (0.483)	0.181 (0.206)	0.083 (0.105)

to the localization properties of the corresponding wave functions.[13,14,15] In particular, Ref. 63, based on a Brownian motion level approximation combined with an assumption concerning the decoupling of the energy levels and eigenfunction correlations, derived the following relation for multifractal eigenstates

$$\chi = \frac{1}{2}\left(1 - \frac{d_2}{d}\right), \tag{10}$$

where d_2 is the correlation dimension of the critical wave functions. According to this result, the spectral compressibility χ should tend to $1/2$ at the limit of very sparse eigenstates $d_2 \to 0$, and not to the Poisson value $\chi = 1$. Although Eq. (10) has been widely confirmed at weak multifractality (weak coupling limit) its validity at strong coupling (small d_2) raises many doubts. More precisely, in Ref. 35, it was analytically shown that at the limit of small b, $\chi \to 1$ for the one-dimensional model (1). This tendency has been also numerically demonstrated in Refs. 35 and 64, and for the Anderson model in $d \geq 4$.[65]

We are therefore especially interested in the calculation of χ for $d = 2$ and 3 in order to check whether or not Eq. (10) adequately describes its behavior at strong coupling $b^d \ll 1$. The compressibility χ can be expressed through the TLCF as

$$\chi = \int_{-\infty}^{\infty} ds\,[R_{d,\beta}(s) - 1]\,. \tag{11}$$

Substitution of Eqs. (4), (5), (8), and (9) into Eq. (11) yields the spectral compressibility for orthogonal ($\beta = 1$) as well as for unitary symmetry ($\beta = 2$)

$$\chi = 1 - c_{d,\beta}\, b^d\,, \tag{12}$$

where $c_{d,1} = 2/a_{d,1}\sqrt{\pi}$ and $c_{d,2} = \sqrt{\pi/a_{d,2}}$. Equation (12) constitutes a generalization to d dimensions of the 1D analytical estimates of Ref. 35. Notice that at the limit of very strong coupling $b^d \to 0$, χ tends to the Poisson value 1 in disagreement with Eq. (10).

An alternative way to directly calculate χ is from the asymptotic behavior of the LNV [Eq. (7)]. We will show that for $b^d \ll 1$, relation (12) is satisfied, thus, giving further support to the proposed relations for the TLCF [Eqs. (8) and (9)].

In Fig. 5, we show the computed $\Sigma^2_{2,1}(\langle n\rangle)$ for the 2D orthogonal ensemble ($\beta = 1$) at different disorders and system sizes: $b^2 = 0.02, L^2 = 40^2$ (right triangles), $b^2 = 0.02, L^2 = 60^2$ (stars), $b^2 = 0.04, L^2 = 40^2$ (down triangles), $b^2 = 0.04, L^2 = 60^2$ (diamonds), $b^2 = 0.08, L^2 = 20^2$ (left triangles), $b^2 = 0.08, L^2 = 60^2$ (squares), $b^2 = 0.1, L^2 = 20^2$ (up triangles), and $b^2 = 0.1, L^2 = 100^2$ (circles). Note that, for each value of b^2, $\Sigma^2_{2,1}(\langle n\rangle)$ is L independent, which is a sign of criticality. There is a clear gradual tendency in the large $\langle n\rangle$ region of $\Sigma^2_{2,1}(\langle n\rangle)$ toward the Poisson limiting result (dashed line) as the inverse coupling constant b^2 of the model is decreased. We have checked that for $\beta = 2$ and for the 3D case the behavior is quite similar. The straight lines, whose slopes correspond to the values of χ, are fits to Eq. (7) with the fitting parameters summarized in Fig. 6.

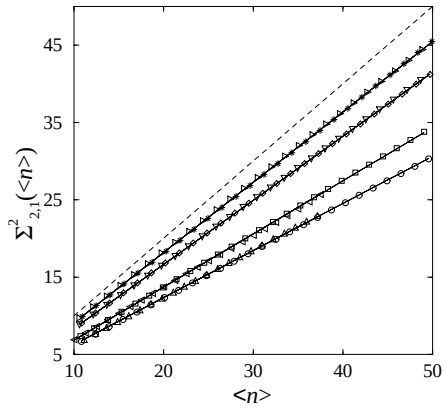

FIG. 5: Level number variance $\Sigma^2_{2,1}(\langle n\rangle)$ for the 2D orthogonal ensemble ($\beta = 1$) at different disorders and system sizes: $b^2 = 0.02, L^2 = 40^2$ (right triangles), $b^2 = 0.02, L^2 = 60^2$ (stars), $b^2 = 0.04, L^2 = 40^2$ (down triangles), $b^2 = 0.04, L^2 = 60^2$ (diamonds), $b^2 = 0.08, L^2 = 20^2$ (left triangles), $b^2 = 0.08, L^2 = 60^2$ (squares), $b^2 = 0.1, L^2 = 20^2$ (up triangles), and $b^2 = 0.1, L^2 = 100^2$ (circles). Solid lines are fits to Eq. (7), and the dashed line corresponds to the Poisson result.

The b^d dependence of the spectral compressibility χ, as obtained from the previous fits, for the 1D (squares), 2D (circles), and 3D (diamonds) model (1) with orthogonal (solid symbols) or unitary symmetry (open symbols) is depicted in Fig. 6. This clearly shows that for almost all values of b^d reported, χ is greater than the maximum value of 0.5 predicted by Eq. (10). The solid lines are fits to the form $\chi = \chi_0 - c_{d,\beta} b^d$ with the fitting parameters $c_{1,1} = 2.27 \pm 0.14$, $c_{1,2} = 2.55 \pm 0.13$, $c_{2,1} = 3.88 \pm 0.12$, $c_{2,2} = 3.90 \pm 0.26$, $c_{3,1} = 4.87 \pm 0.19$, and $c_{3,2} = 5.46 \pm 0.20$. Using these values of $c_{d,\beta}$ and taking into account their relation with the nonuniversal constants $a_{d,\beta}$ of the TLCF, $c_{d,1} = 2/a_{d,1}\sqrt{\pi}$

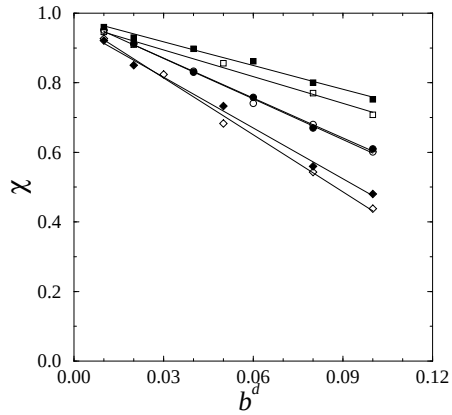

FIG. 6: b^d dependence of the spectral compressibility χ for the 1D (squares), 2D (circles), and 3D (diamonds) models (1) with orthogonal (solid symbols) or unitary symmetry (open symbols). Solid lines are fits to the form $\chi = \chi_0 - c_{d,\beta} b^d$.

and $c_{d,2} = \sqrt{\pi/a_{d,2}}$, we can obtain $a_{d,\beta}$ from a different quantity. The corresponding values are given in brackets in Table I, in which one can appreciate the good agreement with those obtained from the TLCF. Based on these results, one can say that, in the case of strong coupling, the Brownian motion level approximation breaks down and Eq. (10) becomes invalid for all values of d considered.

V. SUMMARY

We present the first numerical results for the two-level correlation function $R_{d,\beta}(s)$ of noninteracting electrons on a d-dimensional disordered system with long-range transfer terms. Models with orthogonal or unitary symmetry at small values of the inverse-coupling constant b^d have been considered. The 1D analytical results [Eqs. (4) and (5)] are confirmed (except for the numerical constants). We also found that the 1D formulas are valid for the 2D and 3D models if the inverse-coupling constant b is replaced by the corresponding to the d-dimensional case b^d. Another important result provided by our numerical calculations is that the spectral compressibility, which is found to be close to 1 in the limit $b^d \to 0$, does not satisfy the relation (10). The proposed Eqs. (8) and (9) are based on numerical results and, at present, should be considered as conjectural. So, further analytical work is needed to check these forms of the TLCF and their origin in the model (1).

Acknowledgments

The author thanks the FEDER and the Spanish DGI for financial support through Project Nos. BFM2003-03800 and FIS2004-03117.

[1] E.P. Wigner, Ann. Math. **67**, 325 (1958).
[2] F.J. Dyson, J. Math. Phys. **3**, 140 (1962).
[3] J.J.M. Verbaarschot and I. Zahed, Phys. Rev. Lett. **70**, 3852 (1993); J. Verbaarschot, *ibid.* **72**, 2531 (1994).
[4] P.W. Brouwer, C. Mudry, B.D. Simons, and A. Altland, Phys. Rev. Lett. **81**, 862 (1998).
[5] C. Mudry, P.W. Brouwer, and A. Furusaki, Phys. Rev. B **59**, 13221 (1999).
[6] C.W.J. Beenakker, Rev. Mod. Phys. **69**, 731 (1997).
[7] Y.V. Fyodorov and H.-J. Sommers, J. Math. Phys. **38**, 1918 (1997).
[8] T. Guhr, A. Müller-Groeling, and H.A. Weidenmüller, Phys. Rep. **299**, 189 (1998).
[9] Y. Alhassid, Rev. Mod. Phys. **72**, 895 (2000).
[10] J. Ambjorn, *Fluctuating Geometries in Statistical Mechanics and Field Theory*, Lectures presented at the 1994 Les Houches Summer School (unpublished).
[11] M.L. Mehta, *Random Matrices* (Academic Press, Boston, 1991).
[12] B.L. Altshuler, I.Kh. Zharekeshev, S.A. Kotochigova, and B.I. Shklovskii, Zh. Eksp. Teor. Fiz. **94**, 343 (1988) [Sov. Phys. JETP **67**, 625 (1988)].
[13] B.I. Shklovskii, B. Shapiro, B.R. Sears, P. Lambrianides, and H.B. Shore, Phys. Rev. B **47**, 11487 (1993).
[14] V.E. Kravtsov, I.V. Lerner, B.L. Altshuler, and A.G. Aronov, Phys. Rev. Lett. **72**, 888 (1994).
[15] B.L. Altshuler and B.I. Shklovskii, Zh. Eksp. Teor. Fiz. **91**, 220 (1986) [Sov. Phys. JETP **64**, 127 (1986)].
[16] A.G. Aronov, V.E. Kravtsov, and I.V. Lerner, Pis'ma Zh. Eksp. Teor. Fiz. **59**, 39 (1994) [JETP Lett. **59**, 40 (1994)]; A.G. Aronov, V.E. Kravtsov, and I.V. Lerner, Phys. Rev. Lett. **74**, 1174 (1995); V.E. Kravtsov and I.V. Lerner, J. Phys. A, **28**, 3623 (1995).
[17] A.G. Aronov and A.D. Mirlin, Phys. Rev. B **51**, R6131 (1995).
[18] Shinsuke M. Nishigaki, Phys. Rev. E **59**, 2853 (1999).
[19] S.N. Evangelou, Phys. Rev. B **49**, R16805 (1994).
[20] Imre Varga, Etienne Hofstetter, Michael Schreiber, and János Pipek, Phys. Rev. B **52**, 7783 (1995).
[21] D. Braun and G. Montambaux, Phys. Rev. B **52**, 13903 (1995).
[22] B. Grémaud and S.R. Jain, J. Phys. A **31**, L637 (1998).
[23] S.R. Jain and A. Khare, Phys. Lett. A **262**, 35 (1999).
[24] E.B. Bogomolny, U. Gerland, and C. Schmit, Phys. Rev. E **59**, R1315 (1999).
[25] G. Auberson, S.R. Jain, and A. Khare, J. Phys. A **34**, 695 (2001).
[26] V.E. Kravtsov and K.A. Muttalib, Phys. Rev. Lett. **79**, 1913 (1997).
[27] Moshe Moshe, Herbert Neuberger, and Boris Shapiro, Phys. Rev. Lett. **73**, 1497 (1994); Jean-Louis Pichard and Boris Shapiro, J. Phys. I **4**, 623 (1994).
[28] K.A. Muttalib, Y. Chen, M.E.H. Ismail, and V.N. Nicopoulos, Phys. Rev. Lett. **71**, 471 (1993).
[29] E. Bogomolny, O. Bohigas, and M.P. Pato, Phys. Rev. E **55**, 6707 (1997).
[30] A.M. García-García and J.J.M. Verbaarschot, Nucl. Phys. B **586**, 668 (2000).
[31] C. Blecken, Y. Chen, and K.A. Muttalib, J. Phys. A **27**, L563 (1994).
[32] A.M. García-García and J.J.M. Verbaarschot, Phys. Rev. E **67**, 046104 (2003).
[33] A.D. Mirlin, Y.V. Fyodorov, F.M. Dittes, J. Quezada, and T.H. Seligman, Phys. Rev. E **54**, 3221 (1996).
[34] A.D. Mirlin, Phys. Rep. **326**, 259 (2000).
[35] A.D. Mirlin and F. Evers, Phys. Rev. B **62**, 7920 (2000).
[36] L.S. Levitov, Europhys. Lett. **9**, 83 (1989); Phys. Rev. Lett. **64**, 547 (1990).
[37] L.S. Levitov, Ann. Phys. (Leipzig) **8**, 697 (1999).
[38] F. Evers and A.D. Mirlin, Phys. Rev. Lett. **84**, 3690 (2000).
[39] V.E. Kravtsov and A.M. Tsvelik, Phys. Rev. B **62**, 9888 (2000).
[40] I. Varga and D. Braun, Phys. Rev. B **61**, R11859 (2000).
[41] Imre Varga, Phys. Rev. B **66**, 094201 (2002).
[42] E. Cuevas, V. Gasparian, and M. Ortuño, Phys. Rev. Lett. **87**, 056601 (2001).
[43] E. Cuevas, M. Ortuño, V. Gasparian, and A. Pérez-Garrido, Phys. Rev. Lett. **88**, 016401 (2002).
[44] E. Cuevas, Phys. Rev. B **66**, 233103 (2002).
[45] O. Yevtushenko and V.E. Kravtsov, J. Phys. A **36**, 8265 (2003).
[46] O. Yevtushenko and V.E. Kravtsov, Phys. Rev. E **69**, 026104 (2004).
[47] E. Cuevas, Europhys. Lett. **67**, 84 (2004).
[48] A.M. García-García, Phys. Rev. B **69**, 245121 (2004).
[49] E. Cuevas, Phys. Rev. B **68**, 024206 (2003).
[50] E. Cuevas, Phys. Rev. B **68**, 184206 (2003).

[51] T.A. Brody, J. Flores, J.B. French, P.A. Mello, A. Pandey, and S.S.M. Wong, Rev. Mod. Phys. **53**, 385 (1981).
[52] V.E. Kravtsov, Ann. Phys. (Leipzig) **8**, 621 (1999).
[53] B.L. Altshuler and L.S. Levitov, Phys. Rep. **288**, 487 (1997).
[54] K.B. Efetov, Adv. Phys. **32**, 53 (1983).
[55] C.C. Yu, Phys. Rev. Lett. **63**, 1160 (1989).
[56] R.N. Bhatt and P.A. Lee, Phys. Rev. Lett. **48**, 344 (1982).
[57] P. Cizeau and J.P. Bouchaud, J. Phys. A **26**, L187 (1993).
[58] A.V. Balatsky and M.I. Salkola, Phys. Rev. Lett. **76**, 2386 (1996).
[59] I.V. Ponomarev and P.G. Silvestrov, Phys. Rev. B **56**, 3742 (1997).
[60] G. Casati and T. Prosen, Physica D **131**, 293 (1999); F. Borgonovi, P. Conti, D. Rebuzzi, B. Hu, and B. Li, *ibid.* **131**, 317 (1999).
[61] E. Cuevas, Phys. Status Solidi B **241**, 2109 (2004).
[62] E. Cuevas, Phys. Rev. Lett. **83**, 140 (1999); E. Cuevas, E. Louis, and J.A. Vergés, *ibid.* **77**, 1970 (1996).
[63] J.T. Chalker, V.E. Kravtsov, and I.V. Lerner, Pis'ma Zh. Eksp. Teor. Fiz. **64**, 355 (1996) [JETP Lett. **64**, 386 (1996)].
[64] M.L. Ndawana and V.E. Kravtsov, J. Phys. A **36**, 3639 (2003).
[65] I.Kh. Zharekeshev and B. Kramer, Ann. Phys. (Leipzig) **7**, 442 (1998).